Acadlore Transactions on Geosciences
https://www.acadlore.com/journals/ATG

# Geoelectrical Characterization of Subsurface Structures in Dala Hill, Kano, Nigeria: A Comparative Study with Ground Magnetic Data

Abba Y. Usman*, Mohammed Saleh, Abubakar G. Shuaibu

Department of Physics, Bayero University Kano, 700241 Kano, Nigeria

* Correspondence: Mohammed Saleh (msaleh.phy@buk.edu.ng)

**Received:** 12-25-2023 **Revised:** 02-21-2024 **Accepted:** 02-28-2024

**Citation:** A. Y. Usman, M. Saleh, A. G. Shuaibu, "Geoelectrical characterization of subsurface structures in Dala Hill, Kano, Nigeria: A comparative study with ground magnetic data," *Acadlore Trans. Geosci.*, vol. 3, no. 1, pp. 37–45, 2024. https://doi.org/10.56578/atg030104.



**Abstract:** A geoelectrical imaging survey, employing resistivity and induced polarization (IP) methodologies, was executed on Dala Hill, Kano, Nigeria, positioned between latitudes $12.008611°\mathrm{N}$ and $12.009722°\mathrm{N}$, and longitudes $8.505833°\mathrm{E}$ and $8.507222°\mathrm{E}$. The objective was to assess and compare findings with prior ground magnetic studies to delineate subsurface geological structures. The survey utilized an ABEM Terrameter SAS 1000 for data acquisition along three distinct profiles encompassing the hill and adjacent areas, with electrode separations fixed at 10 meters. Data processing was conducted using RES2DINV software, revealing resistivity profiles that identified three stratified layers with resistivity values ranging from $300\Omega\mathrm{m}$ to $6798\Omega\mathrm{m}$ for the first layer, $128\Omega\mathrm{m}$ to $744\Omega\mathrm{m}$ for the second, and $4\Omega\mathrm{m}$ to $127\Omega\mathrm{m}$ for the third. IP profiles identified zones of varying chargeability, from $-3.44\mathrm{msec}$ to $19.6\ \mathrm{msec}$. Analysis indicated a consistent positive correlation between zones of high resistivity and low chargeability. For instance, a zone along Profile 1 demonstrated high resistivity values ($2142\Omega\mathrm{m}$ $6798\Omega\mathrm{m}$ ) between $60\ \mathrm{m}$ and $190\ \mathrm{m}$, coinciding with a low chargeability zone ($0.506\mathrm{msec}$ to $2.43\mathrm{msec}$) observed from $20\ \mathrm{m}$ to $100\ \mathrm{m}$ along the profile, equating to depths of $10\ \mathrm{m}$ to $39.6\ \mathrm{m}$. Similar correlations were observed in the subsequent profiles, with significant intersections between high resistivity and low chargeability zones. These areas were interpreted as being rich in iron ore minerals, predominantly magnetite, based on the comparative analysis with standard values of rocks and minerals. The presence of magnetite, known for its high iron content and magnetic properties, underscores the area's potential for steel production. Moreover, the identification of a dyke within the study area corroborates findings from earlier magnetic studies, further validating the geophysical methodology's effectiveness in revealing the shallow subsurface structural settings. This alignment not only substantiates the layered configurations deduced from magnetic studies but also highlights the geoelectrical survey's capability in providing a comprehensive understanding of subsurface geology.

**Keywords:** Chargeability; Resistivity; Induced polarization; Magnetite; Dala Hill; Dyke

## 1 Introduction

Exploration of the Earth's subsurface using geophysical methods has become an important tool for discovering its secrets. These minimally invasive methods serve as an effective investigative tool and provide important information about its structure and organization. Environmental and engineering studies, mining and resource exploration, geological mapping, archaeological research, and many other academic fields are among the problems that have been solved by geophysical techniques [1–4]. The versatility of the methods lies in their ability to measure physical properties at the Earth's surface that are influenced by the internal distribution of these properties within the subsurface. Examples of these properties include density, electrical conductivity, gamma-ray emission, chargeability, magnetism, etc. Geophysical investigations of the earth's interior apply the principles of physics by taking measurements at the surface of the earth that are influenced by the internal distribution of those physical properties. By analyzing these measurements, the physical properties of the earth's interior can be revealed [5]. Electrical tomography techniques are one of the geophysical methods commonly used in geophysical surveys to acquire large amounts of data quickly and also to provide a high-quality image of subsurface structures [6, 7].

Shehu et al. [8] conducted a ground magnetic study to delineate the subsurface structures of Dala Hill. Two classes of anomalies were discovered, with the shallow anomalies correlated with the anthropogenic activities of

ancient settlers and the deep ones associated with internal geologic features. However, all geophysical methods are affected by equivalence and suppression, which is why Shehu et al. [8] recommended the execution of other geophysical studies. Among the methods recommended was ground penetrating radar (GPR) as well as other electrical methods. To provide more complementary information, electrical methods, namely, resistivity, IP, and self-potential, were exploited. The methods have the advantages of controlling the power source, estimating the depth of investigation and determining the lateral extent of influence. In addition, noise can be minimized in the course of data acquisition.

The study area, which is Dala Hill, lies between latitudes $12.008611^{\circ}\mathrm{N}$ and $12.009722^{\circ}\mathrm{N}$ and longitudes $8.505833^{\circ}\mathrm{E}$ and $8.507222^{\circ}\mathrm{E}$. It shares the same geology as Kano State, lying on the rocks of the Basement Complex in northwestern Nigeria. The rocks of the Northern Nigerian Basement Complex consist of three groups: migmatites and high-grade gneisses, derived from the main Birri sedimentary rocks through high-grade metamorphism and granitization; migmatites and finally gneisses during the Pan-African orogeny; and the older granite series intruded during the Pan-African orogeny [9, 10].

Dala Hill rises to a height of about 40 meters above the surrounding area and can be climbed via stairs attached to the front of the hill. Although the hill is rough on the sides due to the weather, it is flat on top. The flat top of the hill is covered by coarse-grained lateritic sediments and a few rocky outcrops, as shown in Figure 1. Lateritic sediments form the uppermost part of the laterite cover. Because the particles are so small, they trap water, giving them a very good water storage capacity. After rainfall, water slowly penetrates the ground. According to the study of Minjibir [11], it covers a land mass of 289,892 square meters. Dala Hill is located in the Dala local government area of Kano State, which is one of the eight local government areas within the Kano metropolis (Figure 2).

**Figure 1.** Top and side views and the foot of the hill occupied by settlements

Generally, the theory of the resistivity method is derived from Ohm's law, which provides the relationship between the magnitudes of the electric field and current density [12–14].

$$J = \sigma E \tag{1}$$

where, $\sigma$ is the conductivity of the medium, $J$ is the current density, and $E$ is the electric field intensity.

However,

$$\rho = \frac{1}{\sigma} \tag{2}$$

where, $\rho$ is the resistivity.

By adopting Ohm's law, it can be shown that the apparent resistivity is given by Eq.(3).

$$\rho = 2\pi r \frac{V}{I} \tag{3}$$

It can also be written as

$$\rho = KR \tag{4}$$

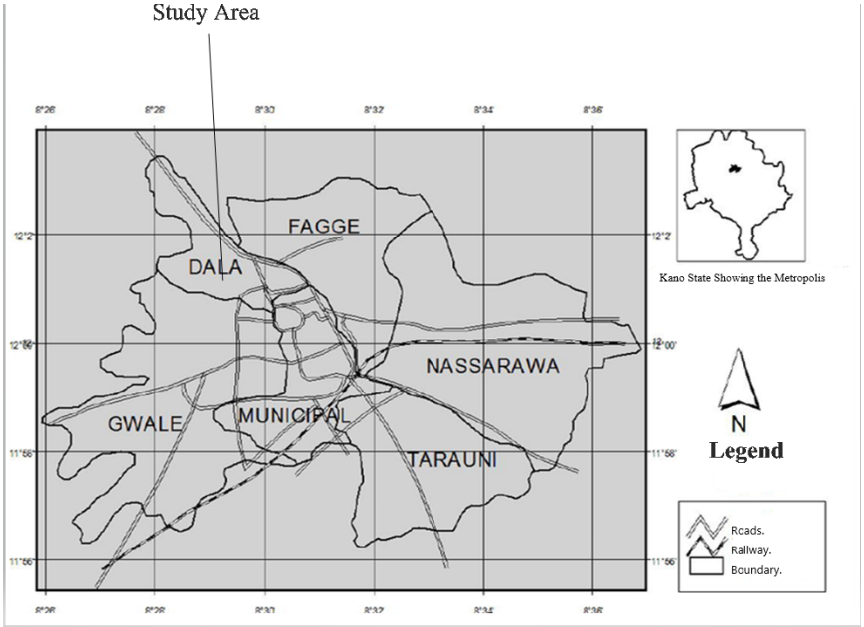


**Figure 2.** Map of Dala local government area showing the study area (GIS LAB GEO DEPT BUK, 2018)

where, $K(K = 2\pi r)$ is the geometric factor that depends on electrode configuration, and $R$ is the actual resistance of the material.

The IP method is based on the ability of certain geological materials, e.g., metallic minerals in a rock, to take on an electrical charge. After an excitation current pulse is introduced into the ground, the measured voltage shows a slow material-dependent decay instead of instantly returning to zero. Their addition to resistivity investigation improves the resolution of resistivity data analysis and can be used to distinguish geological layers that do not respond well to the resistivity method [15–17].

The IP method utilizes the capacitance of the subsurface to identify areas containing conductive minerals dispersed within their host rocks [5, 18, 19].

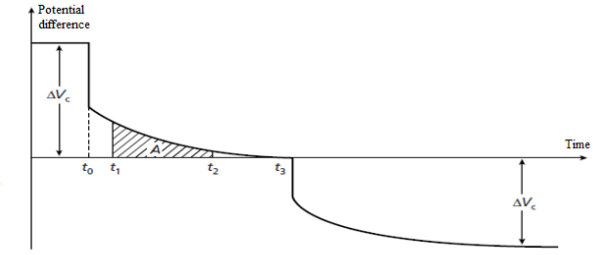


**Figure 3.** The phenomenon of IP [5]

The chargeability $M$ is the parameter most frequently measured, and it is calculated as the area A under the decay curve during a specific time period $(t_l - t_2)$ divided by the steady state potential difference $\Delta V_c$. This is shown in Figure 3 and can be expressed mathematically.

$$M = \frac{A}{\Delta V_c} = \frac{1}{\Delta V_c} \int_{t_1}^{t_2} V(t)dt \tag{5}$$

where, $V(t)$ is the residual voltage at time $t$, and $V_c$ is the steady voltage during the current flow interval.

## 2 Methodology

The imaging was achieved by laying the multi-core cables along the profile with take-outs which were uniformly spaced at 10m spacing. The take-outs were connected to the grounded electrodes via metallic jumpers, as shown in Figure 4. The cables were connected to the Lund imaging device top panel, which was linked to Terrameter SAS

1000 by a cable. The set-up was powered by a 12V, 60W battery and was continuously charged by a 100W solar panel.

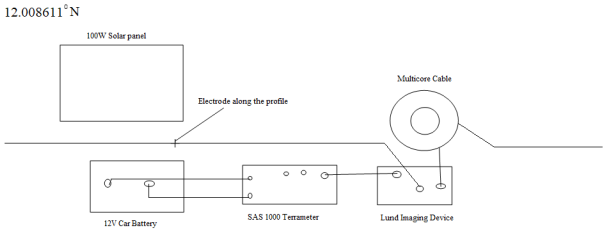


**Figure 4.** Equipment laid out

After switching on the terrameter, the "LUND Imaging System" was selected from the start-up menu. The preferred mode (SP, resistivity, or IP) was selected from the Record Manager and a record file was created for the first profile, with the electrode spacing set to 10m. To mitigate the effects of poor ground contact, the grounding electrodes were filled with saltwater. Additionally, the integrity of the cable connections was regularly evaluated to ensure optimal data acquisition. A current of 1000 mA was selected and the current mode was set to automatic. WENNER L was selected as protocol 1 in order to acquire data from deeper sections of the subsurface. The acquisition systems automatically check the electrode contacts and scan through a pre-defined measurement protocol to check the possibility of current flowing through all the electrodes. Measurements were automatically taken by the equipment and stored in the terrameter. The terrameter took about 20 minutes to complete, taking readings along each profile, with chargeability measurements being the most time-consuming.

The measured apparent resistivity/chargeability data files for all the imaging survey lines were downloaded from the ABEM ES464 Terrameter via cable into a computer in which ABEM file conversion (SAS4000 Utilities) and RES2DINV were installed. The SAS4000 Utilities software was used to convert the original data file (in. s4k format) to the appropriate (.DAT format) input file readable by the inversion software RES2DINV. A total of twelve files were converted (three resistivity files and three IP files). RES2DINV V3.54.44 processed both the resistivity and IP data.

## 3 Results

Interpretation of geophysical data entails translating information acquired from geophysical field measurements into geological terms. To obtain such geological results, available and reliable geological controls were necessary to be sourced for a reliable interpretation of geophysical data. According to the study of Tahir et al. [20], such controls were often obtained from borehole data near the study area, as shown in Table 1. In addition, Table 2 and (Table 3 show the standard values of measured electrical parameters of rocks. This study also exploits the results of previous works within the area and has a good knowledge of its geology.

**Table 1.** Lithology of Kano metropolis obtained using VES [20]

| **Lithology** | **Thickness Range (m)** |
|---|---|
| Top soil | $1.12 - 11.5$ |
| Weathered layer | $5.29 - 54.34$ |
| Fractured layer | $23.18 - 68.60$ |
| Fresh basement | $\infty$ |

**Table 2.** Range of resistivity values of some materials [21]

| **Rock Types** | **Resistivity of Rocks** $(\mathbf{m})$ |
|---|---|
| Clay | $1 - 100$ |
| Weathered bedrock | $100 - 1000$ |
| Granite | $200 - 100000$ |
| Pyrite (ores) | $0.01 - 100$ |
| Magnetite | $0.01 - 1000$ |
| Hematite | $0.01 - 1000000$ |
| Laterite | $60 - 1000$ |

**Table 3.** Chargeabilities of some rocks and minerals [14]

| Minerals/Rocks | Chargeabilities (msec) |
|---|---|
| Pyrite | 13.4 |
| Chalcocite | 13.2 |
| Copper | 12.3 |
| Chalcopyrite | 9.4 |
| Galena | 3.7 |
| Magnetite | 2.2 |

### 3.1 Profile 1

Figure 5 shows the resistivity and chargeability cross sections of Profile 1 . The profile covers a lateral distance of 280 m, from latitude 12.008641°N, longitude 8.506214°E to latitude 12.010795°N, longitude 8.506521°E. The top layer on this profile has a resistivity range of 2142Ωm to 6798Ωm, and the high resistivity could be associated with the intrusion (dyke) observed between 80 m and 190 m marked A1. This intrusion covered an area of size 40 m along the profile and extended deep down beyond 48 m. Towards the end of the profile, a very low resistivity layer with a range of 6.64Ωm to 67.8Ωm was identified and this could be interpreted as a clay deposit due to its low resistivity (Table 2). Along the profile, the chargeability observed can be divided into two main ranges: the first range, which consists of 0.506 to 2.43msec, was observed between 20 m and about 100 m below 10 m to 39.6 m depth; the same range was also observed at 110 m to 200 m trending down to about 27 m. The second chargeability range is 4.35 to 8.19msec, which is observed at 20 to 80 m, approximately from 0 to 10 m depth. The high resistivity zone labeled A1 associated with the dyke intrusion correlates with the low chargeability zone labeled B1, which has a chargeability range of $0.506 - 4.35$msec. This profile shows a good possibility of the presence of magnetite by comparing the resistivity/chargeability values with standard values of minerals (Table 2 and (Table 3).

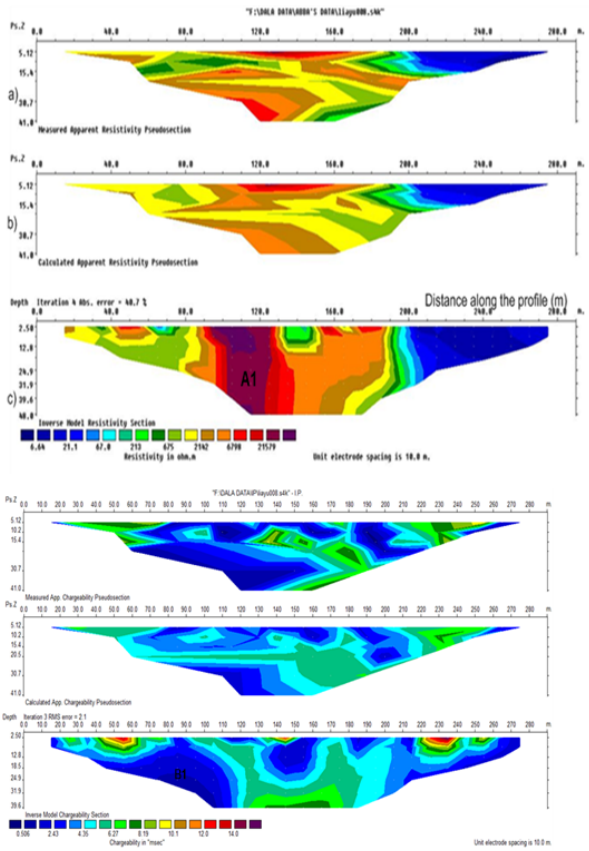


**Figure 5.** Resistivity and chargeability tomography of Profile 1

### 3.2 Profile 2

Figure 6 shows the resistivity and chargeability cross sections of Profile 2 . The profile covers a lateral distance of 360 m with a spacing of 10 m between the electrodes. It starts at latitude 12.008418°N, longitude 8.505930°E, and ends at latitude 12.010909°N, longitude 8.507331°E. This profile reveals three distinct layers. The top layer has a resistivity range of about 1698Ωm to 3874Ωm between 90 m and 250 m along the profile. The second and third layers can be seen at 70 m and 260 m along the profile, with resistivity ranges of 326Ωm to 744Ωm and 12Ωm to 62.7Ωm, respectively. The profile displays two major chargeability ranges. The range, which has a range of 0.911 to 3.58msec at 40 m to 75 m and 120 m to 300 m, has a chargeability that is trending along the profile to a depth of 51.3 m. The second range is 6.24 to 11.6msec and it occurs below 5 m depth at 80 to 130 m and at 170 m to 210 m. The high resistivity zone, which occurs between 80 and 200 m, is marked A3 along the profile and correlates with the low chargeability zone, marked B3. Thus, the observed values at this location fall within the range typically seen for magnetite (Table 2 and (Table 3), suggesting its possible presence.

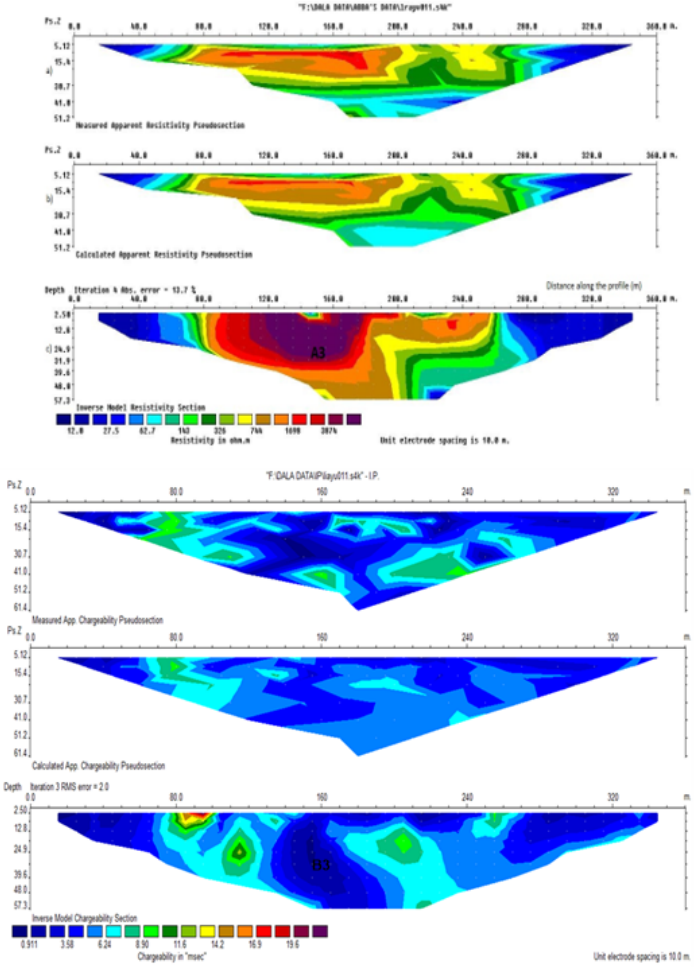


**Figure 6.** Resistivity and chargeability tomography of Profile 2

### 3.3 Profile 3

Figure 7 shows the resistivity and chargeability cross sections of Profile 3 . The profile covers a lateral distance of 260 m with a spacing of 10 m between the electrodes. It starts at latitude 12.008153°N, longitude 8.507970°E, and ends at latitude 12.010082°N, longitude 8.506935°E. The profile reveals three layers. The first layer, which was identified between 70 m and 240 m along the profile and at a depth of about 12 m to 20 m, has a high resistivity range of 651Ωm to 1340Ωm. Thus, the high resistivity is associated with the lateritic nature of the hill. Below the top layer is the second layer, which has a resistivity range of 150Ωm to 319Ωm and is extended to a depth of 48 m. Thus, it was interpreted as a weathered layer containing a sandy clay deposit. The third layer has a low resistivity of less than 100Ωm, as depicted on the profile around 40 m. This could be interpreted as clay. A low chargeability zone having a range of -0.201 to 3.04msec was observed at 190 to 220 m along the profile at a depth of 10 m;

also, the same range was observed at 140 m to 240 m from a depth of about 30 m to 39.6 m. At 70 m to 140 m, a chargeability range of 6.27 to 19.2msec was observed. The high chargeability value observed at 290 to 315 m labeled B1 correlates with the low resistivity zone of the third layer (ranging from 4.93 to 54.1Ωm ) and this high chargeability indicates the possibility of pyrite in the region as the observed values closely agree with the standard values listed in (Table 2 and Table 3).

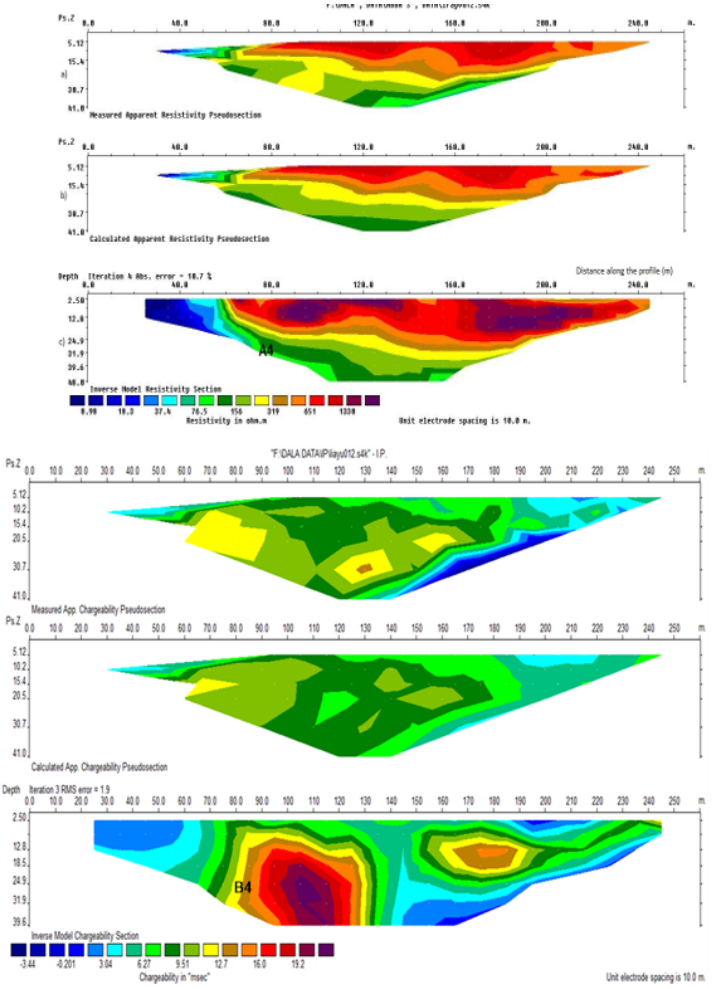


**Figure 7.** Resistivity and chargeability tomography of Profile 3

## 4 Discussion

The inverse sections of the resistivity profiles reveal three layers, with the highest resistivity being the top layer (mainly laterite). The second one contains a weathered basement, and the third one is mainly a highly weathered layer. The IP models reveal the areas of high/low chargeability. The iron ore was identified based on the chargeability model as having zones of low chargeability (0.1-5 msec) for magnetite and hematite as their chargeability values fall within this range (Table 3). Chargeability values of 3-5 msec could indicate an average grade of 10%-20% of iron, while 0.1-3 msec could indicate an average grade of 20%-40% of iron ore [22] . On the basis of this observation, the iron ore within the study area could be inferred to have an average grade of 20%-40%. Considering Profile 1, which was taken from the northwestern part of the study area, an intrusion can be observed at the top layer and extends into the weathered layer, covering a total depth range of 2-48 m. This intrusion is characterized by a high resistivity of iron ore, and seems to contain possible iron ore as it shows a good correlation with low chargeability inversion. Additionally, the presence of this intrusion aligns with findings from the ground magnetic survey conducted by Shehu et al. [8], further supporting the potential for iron ore mineralization in this area. However, as this survey identified potential iron ore deposits successfully, extensive exploration activities may face hindrance due to nearby residential areas. The utilization of the acquired data for knowledge gathering and resource confirmation is crucial, rather than immediate large-scale exploration, as underscored in this context. This study provides a valuable opportunity to enhance the comprehension of historical human activities in the area. The presence of iron ore-associated minerals,

along with low chargeability anomalies, may indicate past utilization of the area by ancient societies for iron ore extraction. Therefore, the geophysical techniques utilized serve as effective and non-destructive investigative tools, especially in constrained environments. This study showcases the applicability of such techniques in confirming the existence of iron-ore-related minerals, potentially offering insights into the resource procurement methods of ancient civilizations.

## 5 Conclusions

Geoelectrical surveys conducted on Dala Hill have utilized resistivity and IP techniques to identify positive correlations between high resistivity and low chargeability zones across three profiles. These findings, in conjunction with the identification of shallow subsurface structures, indicate the possible existence of iron-ore-rich zones that may contain magnetite. Furthermore, a shallow intrusion displaying resistivity characteristics consistent with iron ore has been detected, aligning with previous magnetic studies and providing further evidence for the potential presence of iron ore mineralization. However, the extensive exploration of these areas may be hindered by the presence of nearby residential areas. Despite this limitation, this study underscores the significance of utilizing the acquired geophysical data for confirming the availability of resources and gathering knowledge. Moreover, it has the potential to shed light on past human activities associated with iron ore extraction in the region. The non-destructive geophysical techniques employed in this study have proven to be effective in restricted environments and can serve as valuable tools for confirming the presence of iron-ore-related minerals. Additionally, they offer the possibility of uncovering insights into the resource acquisition practices of ancient civilizations.


## Funding

This research was independently funded by the research team.


## Data Availability

The data used to support the research findings are available from the corresponding author upon request.


## Acknowledgements

We commence by expressing our utmost appreciation to the Almighty for his guidance and blessings that have facilitated our attainment of this momentous achievement. We are genuinely grateful for his divine providence throughout the course of this research expedition.

We would also like to express our sincere gratitude to the following institutions for their invaluable contributions to this study: We extend our heartfelt thanks to Bayero University for generously providing the necessary equipment utilized in the data acquisition process for this research. Their assistance played a pivotal role in carrying out the geophysical surveys. Furthermore, we would like to convey our appreciation to the Kano State Government, specifically the authorities at Gidan Danhausa, for granting us access to the study area situated on Dala Hill. Their cooperation was indispensable in successfully concluding the field investigations.

We are indebted to our families and colleagues for their unwavering encouragement and support throughout the duration of this research project. Their unwavering faith in our work served as a driving force for us to persevere.


## Conflicts of Interest

The authors declare that they have no conflicts of interest.

## References


[1] A. P. Aizebeokhai, "2D and 3D geoelectric resistivity imaging: Theory and field design," *Sci. Res. Essays*, vol. 5, no. 5, pp. 3605–3592, 2010.

[2] T. Dahlin and M. H Loke, "Resolution of 2D Wenner resistivity imaging as assessed by numerical modelling," *J. Appl. Geophys.*, vol. 38, no. 4, pp. 237–249, 1998. https://doi.org/10.1016/s0926-9851(97)00030-x

[3] P. V. Sharma, *Environmental and Engineering Geophysics*. Cambridge University Press, 1997. https://doi.org/10.1017/CBO9781139171168

[4] T. Teixidó, "The surface geophysical methods: A useful tool for the engineer," *Procedia Engi.*, vol. 46, pp. 89–96, 2012. https://doi.org/10.1016/j.proeng.2012.09.450

[5] P. Kearey, M. Brooks, and I. Hill, *An Introduction to Geophysical Exploration (3rd ed.)*, 2002. https://www.wiley.com/en-us/An+Introduction+to+Geophysical+Exploration%2C+3rd+Edition-p-9780632049295

[6] T. Dahlin, "The development of DC resistivity imaging techniques," *Comput. Geosci.*, vol. 27, no. 9, pp. 1019–1029, 2001. https://doi.org/10.1016/s0098-3004(00)00160-6

[7] M. H. Loke and R. D. Barker, "Practical techniques for 3d resistivity surveys and data inversion[1]," *Geophys. Prospect.*, vol. 44, no. 3, pp. 499–523, 1996. https://doi.org/10.1111/j.1365-2478.1996.tb00162.x

[8] A. Shehu, M. Saleh, M. Abubakar Hotoro, and A. Abdulrahim Bunawa, "Application of ground magnetic geophysical method in the delineation of subsurface structures of Dala Hill in Kano ancient city, Northwest Nigeria," *J. Environ. Earth Sci. Res.*, vol. 7, no. 4, pp. 147–152, 2020. https://doi.org/10.18280/eesrj.070404

[9] P. McCurry, "The geology of the Precambrian basement complex of Nigeria," *Episo.*, vol. 12, no. 2, pp. 92–98, 1989.

[10] P. McCurry, *The Geology of the Precambrian to Lower Paleozoic Rocks of Northern Nigeria—A Review*. Geology of Nigeria, Elizabethan Press, 1976.

[11] N. A. Minjibir, "Ancient Kano City Relics and Monuments: Restoration as Strategy for Kano City Development (Master of Landscape Architecture Thesis)." https://www.semanticscholar.org/paper/ANCIENT-KANO-CITY-RELICS-AND-MONUMENTS%3A-RESTORATION-Minjibir/9745faed4322e886aed7e00058ad5d36209d2337

[12] S. H. Ward and G. W. Hohmann, "Electromagnetic theory for geophysical applications. In Electromagnetic methods in applied geophysics—Theory," *Soci. Explo. Geo.*, vol. 1, pp. 131–311, 2012.

[13] P. J. Gibson and D. M. George, *Environmental Applications of Geophysical Surveying Techniques: 2nd edition.*, 2013.

[14] J. Milsom, *Field Geophysics (3rd Edition).* John Wiley and Sons Ltd, Chichester, England., 2003.

[15] T. U. Yusuf, "Overview of effective geophysical methods used in the study of environmental pollutions by waste dumpsites," *An Int. Multi-Discipli. J. Ethiopia*, vol. 10, no. 2, p. 123, 2016. https://doi.org/10.4314/afrrev.v10i2.8

[16] D. T. Amiwero and P. I. Olaseinde, "The evolution of induced polarization method in engineering investigations," *FUPRE J. Sci. Indus. Res.*, vol. 1, no. 2, pp. 1–18, 2017.

[17] A. E. Beck, *Induced polarization*. Macmillan Education London, 1981. https://doi.org/10.1007/978-1-349-16605-3_4

[18] A. Binley and A. Kemna, *DC Resistivity and Induced Polarization Methods*. Springer Netherlands, 2005. http://dx.doi.org/10.1007/1-4020-3102-5_5

[19] H. Burger, A. Sheehan, and C. Jones, *Introduction to applied geophysics: Exploring the shallow subsurface*. Cambridge University Press, 2023. https://doi.org/10.1017/9781009433112

[20] A. G. Tahir, L. Garba, and M. B. Girie, "Subsurface lithology and aquifer zones using vertical electrical sounding method in Kano Metropolis, Northwestern Nigeria," *J. Appl. Geolo. Geophy.*, vol. 2, no. 6, pp. 46–51, 2014.

[21] W. M. Telford, L. Geldart, R. E. Sheriff, and D. A. Keys, *Applied Geophysics (2nd Edition).* Cambridge University Press, 1990.

[22] R. Saad, A. S. Mohamad, and I. Adli, "2-D resistivity and induced polarization (IP) methods for iron ore exploration," *J. EJGE*, vol. 17, pp. 2973–2979, 2012.

**Nomenclature**

| | |
|---|---|
| $K$ | Dimensionless geometric factor |
| $E$ | Electric field intensity $\mathrm{Nm}^{-1}$ |
| $R$ | Resistance, ohms $(\Omega)$ |
| $I$ | Electric current, Amp. (A) |
| $V$ | Potential difference, volt (V) |
| A | Area, $\mathrm{m}^2$ |
| M | Chargeability, milli sec |

Greek symbols

| | |
|---|---|
| $P$ | Resistivity, $\Omega\mathrm{m}$ |
| $\Sigma$ | Electrical conductivity, $\Omega^{-1}\ \mathrm{m}^{-1}$ |

Subscripts

| | |
|---|---|
| $t$ | time |